

### **Synthesis and characterization of di-metallic zeolite Pt-Co composite as potential catalyst for reforming and hydro-sulphurization of gasoline**

#### **Abstract**

Synthesis and characterization of di-metallic zeolite-Pt-Co composite was carried out via hydrothermal treatment, acid leaching of mesoporous-kaolin and calcination of the acidified mesoporous-kaolin. Pt and Co metals were impregnated into the zeolite matrix through thermal reduction of  $\text{H}_2\text{PtCl}_6 \cdot 6\text{H}_2\text{O}$  and  $\text{Co}(\text{CH}_3\text{COO})_2$  at  $550^\circ\text{C}$  for 6 hours using  $(\text{NaBH}_4)$  as reductant with Polyvinylpyrrolidone (PVP) as stabilizer. The results of FTIR indicated absorption bands range of  $1062.3\text{-}74.671\text{ cm}^{-1}$  attributed to tetrahedral stretches for  $\text{AlO}_3$  and  $\text{SiO}$ . A peak at  $779.0\text{ cm}^{-1}$  stretches assigned to Pt and  $650\text{ cm}^{-1}$  due to Co. This may confirm the impregnation of Co and Pt- into the composite. Also, muscovite and quartz interlocking were confirmed at  $1031\text{-}1038\text{ cm}^{-1}$ . The XRD analysis indicated 35 % sanidine  $[(\text{K}, \text{Na})(\text{Si}, \text{Al})_4\text{O}_8]$ , 27 % quartz ( $\text{SiO}_2$ ), 24 % Orthoclase ( $\text{KAlSi}_3\text{O}_8$ ), 8 % Albite ( $\text{NaAlSi}_3\text{O}_8$ ) and 6.3% Muscovite ( $\text{KAl}_2(\text{Si}_3\text{Al})\text{O}_{10}(\text{OH})_2$ ) with sharp peaks of quartz at  $20.8^\circ 2\theta$ , implying crystalline. The results of the Transmission Electron Microscope TEM at 20 nm magnification indicated a uniform morphology with particle size range of 8.22nm - 23.80 nm and average particle size of 16.242 nm. HRTEM result for the synthesized Zeolite Pt-Co composite indicated a particle size range of 3.22 nm -10.27 nm with average particle size of 7.15 nm of disaggregation crystallites morphology. Also, TEM monograph of synthesis Zeolite-Pt-Co indicated a reduced even particle size compared to calcined zeolite clay. Pt enhances isomerization of straight run gasoline with consequent increase in octane number of gasoline while Co aids in hydrosulphurisation.

Key Words: kaolin, Zeolite, catalyst, Calcination, hydrosulphurisation, isomerization

#### **INTRODUCTION**

Ample amount of untapped kaolin deposits is scattered in various parts of Akwa Ibom State and other parts of Nigeria. Zeolites could occur natural or as synthesized crystalline aluminosilicate minerals. Zeolite is made up of three-dimensional structures due to its oxygen bonded background ( $[\text{SiO}_4]_4^-$  and  $[\text{AlO}_4]_5^-$  polyhedral) Victor *et al*, (2020). Zeolite is well defined as crystalline aluminosilicate with different pore sizes which is classified as microporous (pore size smaller than 2 nm), mesoporous (pore size between 2 to 50 nm) and macroporous (pore size larger than 50 nm) Kumaran *et al*, (2019); Lateef *et al*, (2016). Zeolite is used in numerous industrial applications including water purification, petroleum refining especially in fluid catalytic cracking. Hydrocarbon refining (cracking and reforming ) especially fluid catalytic cracking unit is the major consumer of zeolitic catalyst for increasing the quantity of gasoline , octane number enhancement, upgrading of gasoline structure, and production of environmentally friendly hydrocarbon fuel.

According to U.S. Energy Information Administration database for calendar year 2022, Nigeria is ranked 15<sup>th</sup> in crude oil production in the world with 1,316,415 bbl/day. Unfortunately, Nigeria imports all her hydrocarbon fuel due to non-operational refineries. Furthermore, refineries are producing at below installed capacities or are not **working** at all, which has resulted in the inability to refine enough gasoline to meet local consumption Udo *et al.*, (2023), (Udo *et al.*, 2020). Hydrocarbon based fuel are non-biodegradable and non-renewable which may be exhausted Udo *et al.*, (2020). Also, Nigeria untapped zeolitic kaolin are scattered in different locations in Nigeria. Low-cost silica-alumina such as kaolinite Zeolites can be synthesized from kaolinite kaolin via “Hydrogel process”. The structural pattern could be confirmed by the presence of a single characteristic broad band associated with O-H stretching vibrations of the catalytic centers (Si-OH-Al sites) located in the region between 3700-3500 cm<sup>-1</sup> Victor *et al.*, (2020); Isernia, (2013). Highest isomer production was archived with ensemble of Rh bounded with Pt atoms Musselwhite *et al.*, (2013). The Platinum catalysts exhibit high activity and selectivity. Olajire reported that a bimetallic Pt-Cu nanostructure poses greater catalytic oxidative action in desulfurization process

Synthesis of zeolite from clay as a source of silica and alumina from Nigerian kaolin clay has been successfully studied Adeoye *et al.*, (2017); Olaremu *et al.*, (2019); Yusuf *et al.*, (2019). Naturally occurring zeolite is important in many industrial processes due to its environmentally benign nature, low cost and its relative abundance compared to deleterious, expensive and, imported synthetic zeolite. Nigeria has numerous untapped natural kaolin deposits. Unfortunately, for many years now we experience protracted increase in prices of petroleum products especially premium motor spirit (PMS) in Nigeria, with attendant adversative economic consequences. This is because of malfunctioning of all the local refineries in Nigeria, importation of all petroleum products which are sometime adulterated. Pt and Co have high selectivity and catalytic activities with enhance isomerization ability of straight run gasoline and hydrosulphurization respectively. Also, Pt-based bimetallic catalysts display great improved activity, selectivity, and stability compared to monometallic catalyst Shilina *et al.* (2023). Hence, the objective of this study was to design a low cost, ecofriendly, high performance zeolite-Pt-Co composite with enhance isomerization and hydrosulphurization potentials. Pt based catalysts possess a great selectivity to multi branched isomers, with low aromatic compounds production Ghaderi *et al.*, (2021)

## **MATERIALS AND METHODS**

### **Sample Collection**

The kaolin sample used in this study was collected from clay deposits in Ikot Uso Akpan Itam, Itu L.G.A, Akwa Ibom State, using a clean garden fork. The sample was pulverized to enable its usability stored in clean dry plastic container. Ikot Uso Akpan Itam is in Itu Local Government Area, Akwa Ibom State, Nigeria. The study area is bounded in the North and North-East by Odukpani in Cross River State and Arochukwu in Abia State, in the West by Ibiono Ibom and Ikono L.G.A, in the South and South-east by Uyo and Uruan Local Government Areas respectively. Itu has a latitude of 5.203624(5°12'13.05"N) and a longitude of 7.968822(7°58'7.76"E)

### **Hydrothermal Treatment of Kaolin Clay**

In hydrothermal process, 50 g of dried clay sample was added into a 200 **ml** conical flask containing 100 **ml** of deionized water. The mixture was heated at 150 **°C** for one (1) hour with

constant stirring using hot plate with magnetic stirrer, the resulting mixture was filtered and oven dried at 120 °C stored in lid tight containers for further use. Hydrothermal methods can transform kaolin into an ultrafine powder under controlled thermal conditions. The benefits of hydrothermal treatment of kaolin include increased reactants reactivity, low energy consumption, reduced air pollution, easy to control the solution, formational of metastable phases, and unique condensed phases (Johnson and Arshad, 2014).

### Acid leaching of Mesoporous-kaolin

The dried (mesoporous-kaolin) (50 g) prepared in the hydrothermal step was added to a 200 ml conical flask containing 100 ml of 11% hydrochloric acid (HCl). The resulting mixture was heated electrically at 150 °C with constant stirring using magnetic stirrer for one (1) hour and filtered. The solid residue was washed with deionized water until no chloride was detected using AgNO<sub>3</sub>.

### Calcination of the acidified mesoporous -kaolin

The acidified mesoporous -kaolin was oven dried at 120 °C for one (1) hour and calcined at 550 °C for two (2) hours in a muffle furnace and later cooled. The calcined kaolin was stored in a lid tight container and properly labeled. The heating process eliminates water from the mineral kaolinite (Al<sub>2</sub>O<sub>3</sub>·2SiO<sub>2</sub>·2H<sub>2</sub>O), the main constituent of kaolin clay, and collapses the material structure, resulting in an amorphous aluminosilicate (Al<sub>2</sub>O<sub>3</sub>·2SiO<sub>2</sub>), metakaolinite. The process is known as dehydroxylation  $Al_2O_3 \cdot 2SiO_2 \cdot 2H_2O \rightarrow Al_2O_3 \cdot 2SiO_2 + 2H_2O \uparrow$

### Preparation of Zeolite-dimetallic (Zeolite-Pt-Co) Composite

The calcined kaolin prepared from acidified mesoporous -kaolin was used to form Zeolite Pt-Co composite according to Olajire *et al.*, (2017) in the following steps. In the first step, the synthesis of zeolite Pt-Co composite was prepared by mixing 30 mL of 1 M aqueous H<sub>2</sub>PtCl<sub>6</sub>·6H<sub>2</sub>O solution, and 30 mL of 1 M aqueous Co(CH<sub>3</sub>COO)<sub>2</sub> solution with magnetic stirring in a flask. Thirty (30 ml) of 0.002 sodium borohydride (NaBH<sub>4</sub>) was subsequently added to the flask, placed in an ice bath on a stir plate and stirred with addition of 5 g of Polyvinylpyrrolidone (PVP) as stabilizer to prevent aggregation, Olajire *et al.*, (2017). In the second step, ten grams (10 g) of the prepared calcined kaolin catalyst was added into 200 ml conical flask containing 50 ml of deionized water and mixed with the contents in the conical flask in step 1. The mixture was heated for 1 hour at 150 °C using hot plate and oven-dried at 120 °C for 1 hour for reduction process. The dried mesoporous clay composite Zeolite-Pt-Co composite was further calcined at 550 °C for 5 hours in a muffle furnace to and stored in a labeled lid tight container.

### Characterization of the synthesized Zeolite-Pt-Co

The functional groups profile and molecular finger print of the synthesized zeolite-Pt-Co composite was analyzed using Agilent Technologies Cary 630 FTIR, Benchtop FTIR Spectrometer with depth 26 cm, height 16 cm, power requirement- 100-240 VAC, 50/60 Hz, Resolution- ≤ 2 cm<sup>-1</sup>, sample type-powder couple with MicroLab Pharma Software. Unique Ux-30 XRF spectrophotometer was to analyze individual elementals and compound present in the composite. The crystalline phase identification (phase ID), quantification and percent (%) crystallinity, of the synthesized zeolite-Pt-Co composite were carried out using Rigaku Miniflex Benchtop powder X-ray Diffraction (XRD) instrument. Core attribute- 600 W X-ray tube, D/teX

Ultra silicon strip detector, Core dimensions-620 (W) x 722 (H) x 460 (D) mm, Power requirements-1Ø, 100-240 V 50/60 Hz mounted with External PC, MS Windows OS, SmartLab Studio-II software.

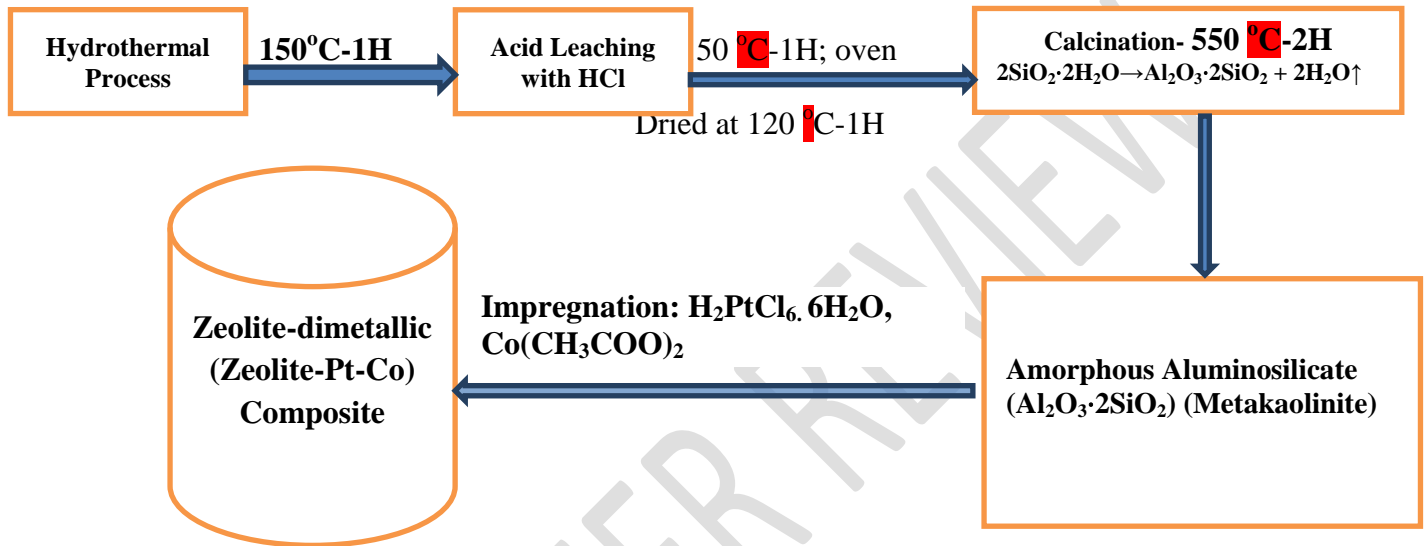


Figure 1: Flow chart for synthesis of Zeolite-dimetallic (Zeolite-Pt-Co) Composite

## RESULTS AND DISCUSSIONS

The results of XRD, FTIR, TEM and XRF of the synthesized Zeolite-Pt-Co composite, Figure 1 are as presented in Figure 2- Figure 7 and Table 1 XRD analysis of the Zeolite-Pt-Co. From the results of XRD data Fig. 2 -Fig 3, the Zeolite-Pt-Co composite produced contained 35% sanidine  $[(K,Na)(Si,Al)_4O_8]$  Haldar and Josip (2014), 27 % quartz ( $SiO_2$ ), 24 % Orthoclas ( $KAlSi_3O_8$ ), 8% Albite ( $NaAlSi_3O_8$ ) and 6.3% Muscovite ( $KAl_2(Si_3Al)O_{10}(OH)_2$ ). Also, the X-ray diffraction patterns of the Zeolite-Pt-Co composite indicated sharp peaks for quartz at  $20.8^\circ 2\theta$ , implying that the composite is crystalline. The peak at  $2\theta = 3.4^\circ$  is associated with d220 reflection the peaks  $6.16^\circ$ ,  $15.88^\circ$ ,  $26.08^\circ$ , and  $30.7^\circ$  depict the HY zeolite Anbia *et al*, (2015), Peng *et al*, (2016), Ghaderi *et al*, (2021). In a similar study by Yusuf *et al*, (2019) XRD data indicated two peaks corresponding to the kaolinite and quartz in Elefun Kaolin.

Phase Data View

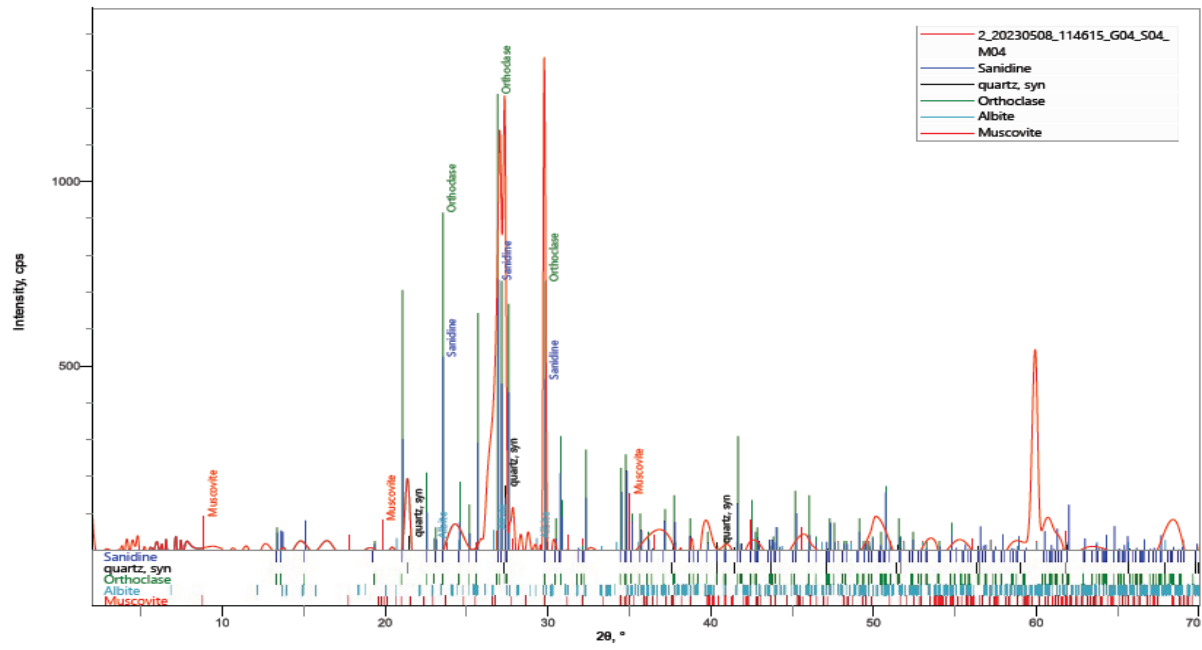


Figure 2: XRD phase data view of Zeolite-Pt-Co composite

Plot of results

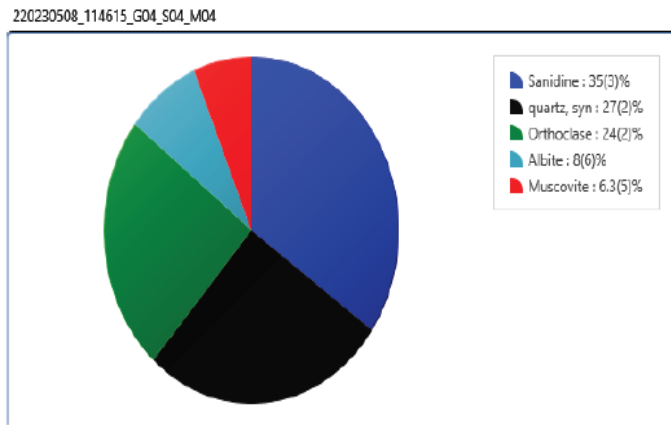


Table of results

Dataset / Weight Fraction, wt%	Value, Unit	Sanidine	quartz, syn	Orthoclase	Albite	Muscovite
2_20230508_114615_G04_S04_...	0	35(3)	27(2)	24(2)	8(6)	6.3(5)

Figure 3: Percentage composition of Sanidine, quartz, Orthoclase, Albite and Muscovite

### FTIR spectroscopy Analysis.

The results of FTIR spectroscopy analysis of the synthesized Zeolite-Pt-Co composite are as presented in Figures 4-5. From the FTIR data results, the absorption bands ranges observed at  $1062.3-74.671\text{ cm}^{-1}$  is attributed to tetrahedral stretches for  $\text{AlO}_3$  and  $\text{SiO}$  Kumaran *et al*, (2019). Ezra *et al*, (2021) reported  $1067.44\text{ cm}^{-1}$  absorption band for symmetric stretching vibration of Si-O-Si bond. The  $1062.3\text{ cm}^{-1}$  stretches could also be attributed to Si-O quartz. The result of FTIR of the calcined kaolin clay was in line with the research of Bhaskar *et al*, (2010) who confirmed that “the main peaks in the infrared spectra reflected Al-OH, Al-O and Si-O functional groups in the high frequency stretching and low frequency bending modes”.  $4000-650\text{ cm}^{-1}$  stretches could be associated with Co-O and Pt vibrations. This may confirm the impregnation of Co and Pt into the synthesized Zeolite-Pt-Co composite Abubakar *et al*, (2023). Shilina *et al*, (2023), Eurov *et al*, (2022) observed a Co small band near  $669\text{ cm}^{-1}$  due to stretching vibrations of the metal–oxygen bond in  $\text{Co}_3\text{O}_4$ . Cobalt serves as catalyst for hydrodesulfurization in petroleum refining and can enhance catalytic oxidation of hydrocarbons. The wave number  $3678.9\text{ cm}^{-1}$  and  $3596.5\text{ cm}^{-1}$  (Figure 4) may be assigned to Al–O–H stretching and OH Stretching - Crystalline hydroxyl respectively. The obtained FT-IR in this study is congruent with the studies of Nguyen *et al*, 2019 and Saikia *et al*, (2010). Also, Jiangyong *et al*, 2016 opined that zeolite-cobalt supported catalyst, exhibited considerably higher gasoline selectivity and produced more *iso*-paraffins. The synthesized zeolite-Pt-Co composite in this work can provide a confined reaction area for increased diffusion efficiency with a good reduction performance.

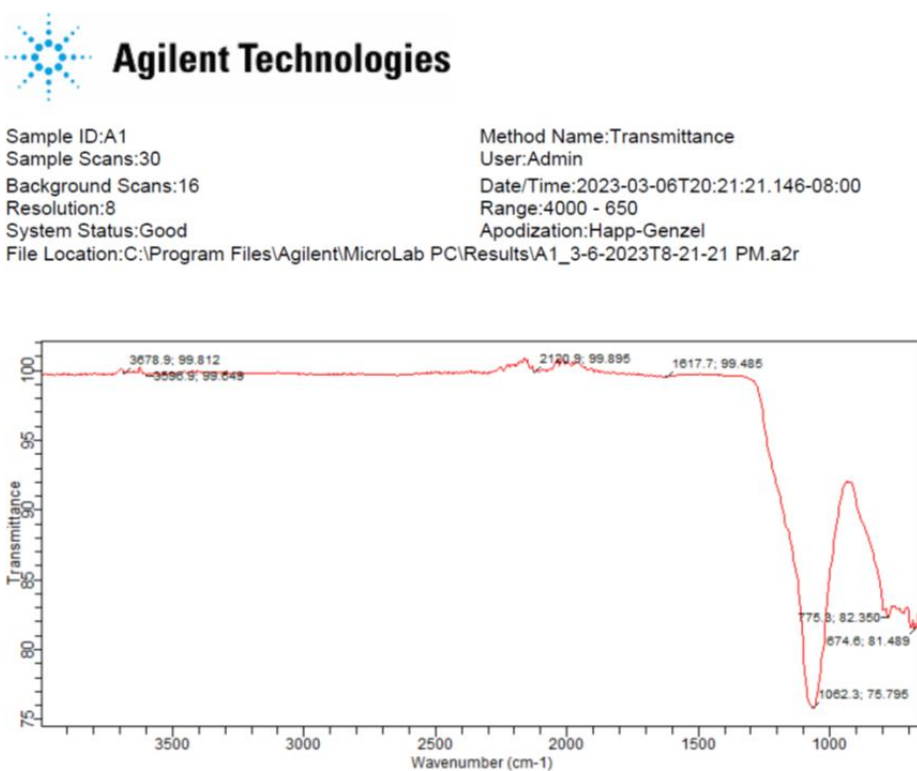


Figure 4: FTIR of calcined kaolin clay

Sample ID:2	Method Name:Transmittance
Sample Scans:30	User:Admin
Background Scans:16	Date/Time:2023-05-09T09:33:15.262-07:00
Resolution:8	Range:4000 - 650
System Status:Good	Apodization:Happ-Genzel
File Location:C:\Program Files\Agilent\MicroLab PC\Results\2_5-9-2023T9-33-15 AM.a2r	

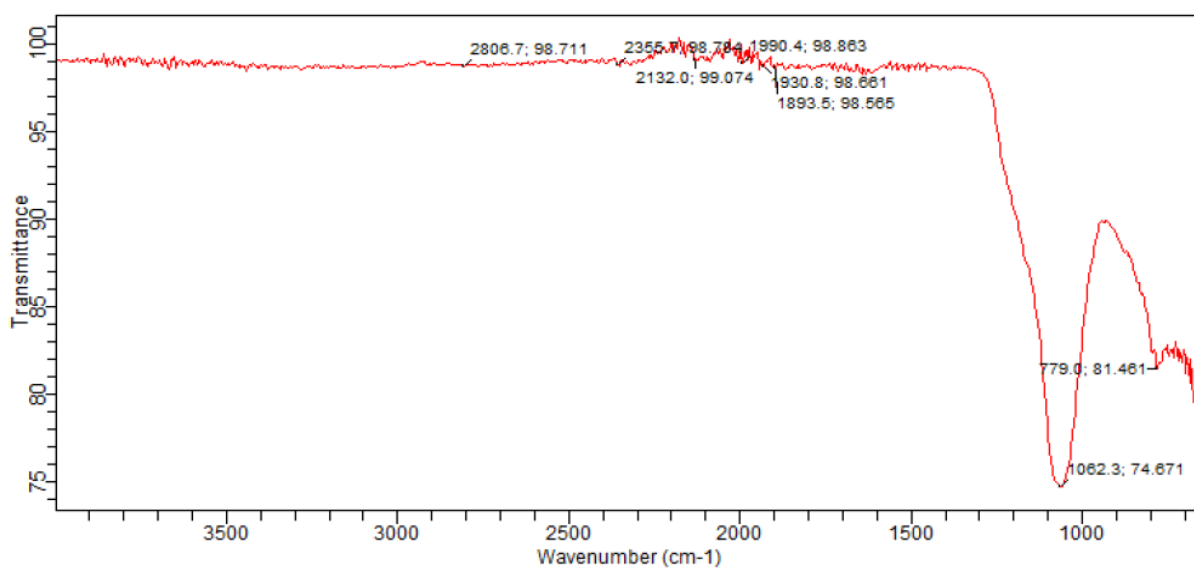


Figure 5: FTIR of Zeolite-Pt-Co composite

High Resolution Transmission Electron Microscopy (HRTEM) of the Calcined zeolite and synthesis zeolite-Pt-Co composite:

High Resolution Transmission Electron Microscopy (HRTEM) was used to characterize the lattice arrangement and crystallinity of the calcined zeolite and synthesis Zeolite-Pt-Co composite structures. The results are as presented in Figure 6 and Figure 7. The results of the Transmission Electron Microscope TEM at 20nm magnification indicated a uniform morphology with particle size range of 8.22 nm - 23.80 nm and average particle size of 16.242 nm. Comparatively, the HRTEM result for the synthesized Zeolite Pt-Co composite indicated a particle size range of 3.22 nm -10.27 nm with average particle size of 7.15 nm with disaggregation crystallites. The TEM monograph of synthesis Zeolite-Pt-Co indicated a smaller particle size Figure 7 compared to calcined zeolite clay Figure 6. The reduction in average particle size of 16.242 nm for calcined zeolite to 7.15 nm in synthesized Zeolite-Pt-Co

composite could implies that Pt and Co were successfully impregnated into the synthesized composite with production of nan- particle size Gajendran (2017). In related study by Bingxue *et al*, (2022) PtCo/C nanoparticle size was less than 5 nm, showing its high oxygen reduction reaction activity potential. The TEM image of the Zeolite-Pt-Co composite Figure 7 indicates that Co and Pt are evenly distributed on the synthesized zeolite composite. In a related research by Olajire *et al*, (2017), it was reported that The Pt and Cu nanostructures revealed exceedingly even morphology with sizes range between 1.87 and 2.38 nm and average particles size of  $2.12 \pm 0.21$  nm. Yesmurzayeva *et al*, (2016) reported a reduced particle size using of 0.235 nm and 0.208 nm using gold and the copper nanoparticle respectively. Platinum (Pt) atoms can function as catalyst for isomerization of hydrocarbons, Musselwhite *et al*, (2013). According to Zirong *et al*, 2021, incorporation of Pt nanocomposites display much improved performance in durability and high efficiency. The TEM image also, in similar work by Nandhi and Gajendran (2017).

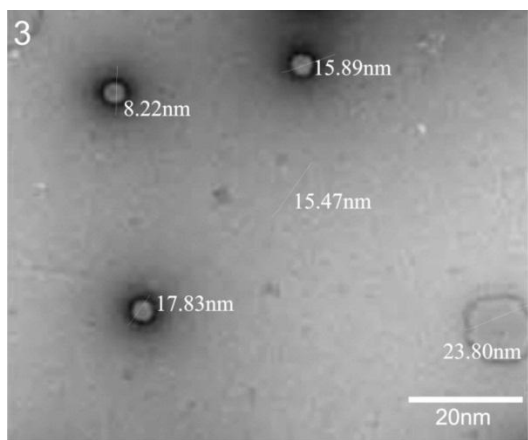


Figure 6: TEM monograph of Calcined kaolin

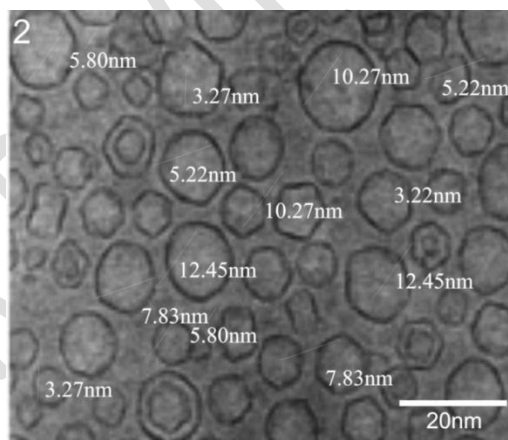


Figure 7: TEM monograph of Zeolite-Pt-Co composite

The result of the XRF analysis of the calcined kaolin revealed  $\text{SiO}_2$  (63.001 %),  $\text{Al}_2\text{O}_3$ (31.017 %),  $\text{K}_2\text{O}$  (2.163 %),  $\text{TiO}_2$  (2.220 %) and  $\text{Fe}_2\text{O}_3$ (1.850) as major chemical compositions with 1.850 %, 2.220 %, 2.163 % of  $\text{Fe}_2\text{O}_3$ ,  $\text{TiO}_2$ ,  $\text{K}_2\text{O}$  as trace impurities. In a related work by Abiodun *et al*, (2023), 48.62 %  $\text{SiO}_2$ , 31.45%  $\text{Al}_2\text{O}_3$  and 4.08  $\text{Fe}_2\text{O}_3$  were recorded in a metakaolin at 500 °C . Percentages of the major individual element present in calcined clay were oxygen 49.250, aluminium 15.956 and silicon 28.314 % Table 1. Comparatively, the XRF analysis recorded  $\text{SiO}_2$  (63.001 %),  $\text{Al}_2\text{O}_3$  (31.017%),  $\text{PtO}_2$  (6.011 %), with trace amount of  $\text{Cr}_2\text{O}_3$ , (0.770 %),  $\text{Co}_3\text{O}_4$  (0.002 %),  $\text{Fe}_2\text{O}_3$  (0.770 %),  $\text{V}_2\text{O}_5$  (0.106 %). The concentrations of individual elements in the synthesized Zeolite-Pt-Co composite were Zn (11.134 %). Fe(34.158), Sb (4.571 %), Si (30.280 %), Al (18.010 %), Pt (29.674 %), O (37.000 %), S (1.015), K (1.267 %) and Co (32.834 %) respectively. Table1. The result of XRF together with XRD and FTIR indicated that Pt and Co were successfully impregnated in the synthesis Zeolite-Pt-Co composite Table 1, Figures 2 and 3. In related research, Shilina *et al*, (2023) deposited Pt and Co Pt-Co/ZSM-5 Catalysts using laser electrodispersion on Co-modified ZSM-5 prepared by the  $\text{Co}(\text{CH}_3\text{COO})_2$  impregnation.

Table 1: XRF results of calcined and Zeolite-Pt-Co composite

Calcined Kaolin		Zeolite-Pt-Co Composite	
components	concentrations	Components	Concentrations
SiO <sub>2</sub>	63.001	SiO <sub>2</sub>	63.001
V <sub>2</sub> O <sub>5</sub>	0.106	V <sub>2</sub> O <sub>5</sub>	0.106
Cr <sub>2</sub> O <sub>3</sub>	0.069	Cr <sub>2</sub> O <sub>3</sub>	0.069
MnO	0.013	MnO	0.013
Fe <sub>2</sub> O <sub>3</sub>	1.850	Fe <sub>2</sub> O <sub>3</sub>	0.770
Co <sub>3</sub> O <sub>4</sub>	0.005	Co <sub>3</sub> O <sub>4</sub>	0.002
NiO	0.007	NiO	0.007
CuO	0.028	CuO	0.028
Nb <sub>2</sub> O <sub>3</sub>	0.010	Sn	11.134
MoO <sub>3</sub>	0.002	Fe	34.158
WO <sub>3</sub>	0.000	Sb	4.571
P <sub>2</sub> O <sub>5</sub>	0.000	Mn	ND
SO <sub>3</sub>	0.198	Ni	ND
CaO	0.336	Co	32.834
MgO	0.000	Cr	34.158
K <sub>2</sub> O	2.163	Pt	29.674
BaO	0.113	Al <sub>2</sub> O <sub>3</sub>	31.017
Al <sub>2</sub> O <sub>3</sub>	31.017	PtO	6.011
Ta <sub>2</sub> O <sub>5</sub>	0.027	Cl	1.000
TiO <sub>2</sub>	2.220	Si	30.280
ZnO	0.010	Al	18.010
Ag <sub>2</sub> O	0.007	O	37.000
Cl	0.686	Mg	0.012
ZrO <sub>2</sub>	0.131	S	1.015
SnO <sub>2</sub>	0.000	K	1.267
O	49.250		
Al	15.956		
Si	28.314		

## CONCLUSION

Synthesis and characterization of di-metallic zeolite Pt-Co composite was carried out via Hydrothermal Treatment, Acid leaching of Mesoporous-kaolin and Calcination of the acidified mesoporous –kaolin. The Pt and Co metals were impregnated into the zeolite matrix through reduction of H<sub>2</sub>PtCl<sub>6</sub>.6H<sub>2</sub>O and Co(CH<sub>3</sub>COO)<sub>2</sub> at 550 °C for 6 hrs using (NaBH<sub>4</sub>) as reductant with Polyvinylpyrrolidone (PVP) as stabilizer. The results of FTIR indicated absorption bands range of 1062.3-74.671 cm<sup>-1</sup> attributed to tetrahedral stretches for AlO<sub>3</sub> and SiO. A peak at 779.0 cm<sup>-1</sup> stretches assigned to Pt and 650 cm<sup>-1</sup> due to Co. This may confirm the impregnation of -Co and Pt- into the synthesis Zeolite-Pt-Co composite. Muscovite and quartz interlocking might remain at 1031-1038 cm<sup>-1</sup>. The XRD analysis indicated 35 % sanidine ((K,Na)(Si,Al)<sub>4</sub>O<sub>8</sub>)27%

quartz ( $SiO_2$ ), 24 % Orthoclas ( $KAlSi_3O_8$ ), 8 % Albite ( $NaAlSi_3O_8$ ) and 6.3 % Muscovite ( $KAl_2(Si_3Al)O_{10}(OH)_2$ ) with sharp peaks of quartz at  $20.8^\circ 2\theta$ , implying crystalline. The results of the Transmission Electron Microscope TEM at 20nm magnification indicated a uniform morphology with particle size range of 8.22nm - 23.80 nm and average particle size of 16.242 nm. HRTEM result for the synthesized Zeolite Pt-Co composite indicated a particle size range of 3.22 nm -10.27 nm with average particle size of 7.15 nm of disaggregation crystallites morphology. Also, TEM monograph of synthesis Zeolite-Pt-Co indicated a reduced even particle size compared to calcined zeolite clay. Pt enhances isomerization of straight run gasoline with consequent increase in octane number of gasoline while Co aids in hydrosulphurisation. Also, the synthesized zeolite-Pt-Co composite in this work can provide a confined reaction area for increased diffusion efficiency with a good reduction performance.

**Funding:** This research was funded by Tertiary Education Trust Fund (TETFUND)

**Acknowledgements:** The authors acknowledge the contribution of Tertiary Education Trust Fund (TETFUND) and Management of Akwa Ibom State University for funding this project.

## References

**Abiodun, Y.O ; Orisaleye, J.I. and Adeosun, S.O. (2023).** Effect of Calcination Temperatures of Kaolin on Compressive and Flexural Strengths of Metakaolin-Concrete . Nigerian Journal of Technological Development, 20 (1): 33-43.

**Anbia, M.; Kargosha, K. and Khoshbooei, S. (2015).** Heavy metal ions removal from aqueous media by modified magnetic mesoporous silica MCM-48. Chem Eng Res Des. 93: 779–88.

**Abubakar, S. Y.; Alhassan, M.; Lawal, I S.; Shehu, Y. and Muhammad H. (2023).** Studies of neat kaolin and cobalt (iii) oxide doped kaolin for Heterogeneous Catalysts Development Using Fourier Transform Infrared Spectroscopy. Science World Journal 18(1), 1597-6343

**Bingxue, H.; Xinlei, L.; Ziheng Zheng, R. T.; Qi Zhang, M. G.; Chengcheng, W.; and Zanxiong T. (2022).** An Efficient Electrocatalyst (PtCo/C) for the Oxygen Reduction Reaction, Catalyst 12 (794). [https:// doi.org/10.3390/catal12070794](https://doi.org/10.3390/catal12070794)

**Bhaskar J. S. and Gopalakrishnarao, P.(2010).** Fourier Transform Infrared Spectroscopic Characterization of Kaolinite from Assam and Meghalaya, Northeastern India. J. Mod. Phys. 1: 206-210

**Eurov, D.A.; Rostovshchikova, T.N.; Shilina, M.I.; Kirilenko, D.A.; Tomkovich, M.V.; Yagovkina, M.A.; Udalova, O.V.; Kaplin, I.Y.; Ivanin, I.A. and Kurdyukov, D.A. (2022).**

Cobalt oxide decorated porous silica particle Structure and activity relationship in the catalytic oxidation of carbon monoxide. *Appl. Surf. Sci.* 579 (152121).

**Ezra, A.; Zaccheus.; Shehub, D.; Wilson, L.; Kennedy, P.; Yoriyoa, R. K. and Nsor, C.A.(2021).** Novel developments of ZnO/SiO<sub>2</sub> nanocomposite: a nanotechnological approach towards insect vector control. *J. Nig. Soc. Phys. Sci.* 3, 262–266

**Jiangyong Liu 1, Dan Wang, Jian-Feng Chen, Yi Zhang (2016).** Cobalt nanoparticles imbedded into zeolite crystals: A tailor-made catalyst for one-step synthesis of gasoline from syngas. *International Journal of Hydrogen Energy* 41(47): 21965-21978

**Johnson, E.B.G., Arshad, Sazmal E. (2014).** Hydrothermally synthesized zeolites based on kaolinite: A review *Applied Clay Science* 97–98: 215-221

**Peng, R.; Wu, C.M.; Baltrusaitis, J.; Dimitrijevic, N.M.; Rajh, T. and Koodali, R.T. (2016).** Solar hydrogen generation over CdS incorporated in Ti-MCM-48 mesoporous materials under visible light illumination. *Int J Hydrogen Energy.* 41(7):4106–19.

**Ghaderi, Z.; Peyrovi, M. H. and Parsafard, N. (2021).** n-Heptane isomerization activities of Pt catalyst supported on micro/mesoporous composites. *BMC Chemistry*, 15(61): 1-8.

**Musselwhite, N.; Alayoglu, S. and Melaet, G. (2013).** Isomerization of n-Hexane Catalyzed by Supported Monodisperse PtRh Bimetallic Nanoparticles. *Catal Lett* 143: 907–911  
<https://doi.org/10.1007/s10562-013-1068-5>

**Yesmurzayeva, N.; Tursunova, R.; Nakypova, S.; Selenova B. and Kudaibergenov S. (2016).** Synthesis and Characterization of Catalysts Based on Bimetallic Nanoparticles 6th International Conference on Nanomaterials: Applications and Properties (NAP) 1-4.

**Prabhu, N Gajendran, T. (2017).** Green Synthesis of Noble Metal of Platinum Nanoparticles from *Ocimum sanctum* (Tulsi) Plant- Extracts. *IOSR Journal of Biotechnology and Biochemistry*, 3(1): 107-112.

**Olajire, A. A.; Kareem, A. and Olaleke, V (2017).** Green synthesis of bimetallic Pt-Cu nanostructures for catalytic oxidative desulfurization of model oil. *J Nanostruct Chem*, 7:159–170.

**Shilina, M.; Krotova, I.; Nikolaev, S.; Gurevich, S.; Yavsin, D.; Udalova, O. and Rostovshchikova, T. (2023).** Highly Effective Pt-Co/ZSM-5 Catalysts with Low Pt Loading for Preferential Co Oxidation in H<sub>2</sub>-Rich Mixture. *Hydrogen* 4, 154–173. <https://doi.org/10.3390/hydrogen4010011>

**Thi, K. L. N.; Ngoc, D. N.; Van, P. D.; Dinh, T. P.; Thai, H. T. and Quoc, H. N. (2019).** Synthesis of Platinum Nanoparticles by Gamma Co-60 Ray Irradiation Method Using Chitosan as Stabilizer. *Advances in Materials Science and Engineering*, 2019:1-5  
<https://doi.org/10.1155/2019/9624374>

**Palanivel, S. and Natarajan, S. (2012).** Cobalt Recovery from Waste Catalysts (Petroleum Refining Industry from Gujarat) *Open Journal of Metal*, 2: 24-30 [DOI:10.4236/ojmetal.2012.21004](https://doi.org/10.4236/ojmetal.2012.21004)

**Udo, G.J.; Awaka-Ama, J.J.; Nyong, A.E.; Ekanem, A.N. and Igwe, R.C. (2023).** GC-MS Analysis of Artisanal Refined and Regular Automotive Gasoline: Comparative Study of Quality. *International Journal of Novel Research and Development*. 8(1): 2456-4184

**Udo, G.J.; Awaka-Ama, J.J.; Uwanta, E.J.; Ekwere, I.O.; and Chibueze, I.R. (2020).** Comparative Analyses of Physicochemical Properties of Artisanal Refined Gasoline and Regular Automotive Gasoline. *Front. Chem.* 8:753. doi: 10.3389/fchem.2020.00753

**Udo, G. J.; Eteson, U.M.; Awaka-Ama J.J., Nyong, A.E. and Uwanta, E.J. Uwanta (2020).** GCMS and FTIR Spectroscopy Characterization of Luffa Cylindrica Seed Oil and Biodiesel Produced from the oil. *Communication in Physical Sciences* 2020, 5(3): 378-390

**Yusuf, E.O; Efevbokhan, V. E. and Babalola, R. (2019).** Development and Characterization of Zeolite-A from Elefun Kaolin *Journal of Physics: Conference Series* 1378,1-8  
doi:10.1088/1742-6596/1378/3/032016

**Zirong Li, Tingting Cheng , Lei Bai and Aiqin, Ye (2021).** Pt-Pd Bimetallic Nanocomposites Catalyst Formed on Graphene Surface: Preparation and high-performance for Methanol Electro-Oxidation. *Int. J. Electrochem. Sci.*, 16 :1-11. doi: 10.20964/2021.08.10